

國立交通大學

機械工程學系

碩士論文

圓柱形腔體內部散熱鰭片與機械震盪結
合之自然對流研究

Natural convection in a cylindrical enclosure
with pin fins and mechanical vibrations

研究生：許顥儒

指導教授：劉耀先 博士

中華民國一〇二年七月

圓柱形腔體內部散熱鰭片與機械震盪結合之自然對流研究

Natural convection in a cylindrical enclosure with pin fins and
mechanical vibrations

研究生：許顥儒

Student: Hao-Ju Hsu

指導教授：劉耀先 博士

Adviser: Yao-Hsien Liu

國立交通大學

機械工程學系

碩士論文

A Thesis

Submitted to Institute of Mechanical Engineering

College of Engineering

National Chiao Tung University

In Partial Fulfillment of the Requirements

for the Degree of

Master of Science

In

Mechanical Engineering

Jul. 2013

Hsinchu, Taiwan, Republic of China

圓柱形腔體內部散熱鰭片與機械震盪結合之自然對流研究

Natural convection in a cylindrical enclosure with pin fins and
mechanical vibrations

學生：許顥儒

指導教授：劉耀先

國立交通大學機械工程學系碩士班

摘要

自 1970 年代石油危機開始，世界各國慢慢注意到發展再生能源的必要性，以減緩對石油等傳統能源的依賴，如太陽能、風力、地熱以及波浪能等等。這些大自然的能源可謂取之不盡，用之不竭。

近年來台灣在這方面發展也逐漸步上軌道，本文的實驗原型是來自工業技術研究院 20 kW 等級之波浪發電機組，因波浪發電機組內含大量電子零件，而機組本身是完全封閉之腔體，散熱就變成一大課題。

本研究的目的是以實驗的方法探討類似波浪發電機組內部的圓柱形中空腔體，模擬波浪發電機組內部發熱源，並以步進馬達以及震盪機構模擬波浪發電機組在海面上載浮載沉的運轉條件，探討腔體震盪對自然對流熱傳的影響，研究不同的腔體高度($H=2.5\text{cm}, 5\text{cm}$)、震盪頻率($f=1\text{Hz}, 2\text{Hz}$)、Rayleigh number($Ra=5 \times 10^4 \sim 6 \times 10^5$)以及散熱鰭片對自然對流的影響。經由實驗得到的結果可看出，因震盪而增加

熱傳的效果($E_v(\text{Nu})$ ，為 1.0~1.1)明顯比因加入散熱鰭片而增加的熱傳($E_f(\text{Nu})$ ，為 1.1~1.4)還少，因此可判斷在此震盪條件下，腔體內部的自然對流受到震盪因素影響的程度是不明顯的。

關鍵字:自然對流、波浪發電、震盪、密閉腔體、散熱鰭片



Student: Hao-Ju Hsu Adviser: Prof. Yao-Hsien Liu

Institute of Mechanical Engineering

National Chiao Tung University

ABSTRACT

Since the energy crisis in 1970s, the attention in developing renewable energy such as solar energy, wind energy, geothermal energy and wave energy has increased worldwide in order to reduce the dependence on traditional energy.

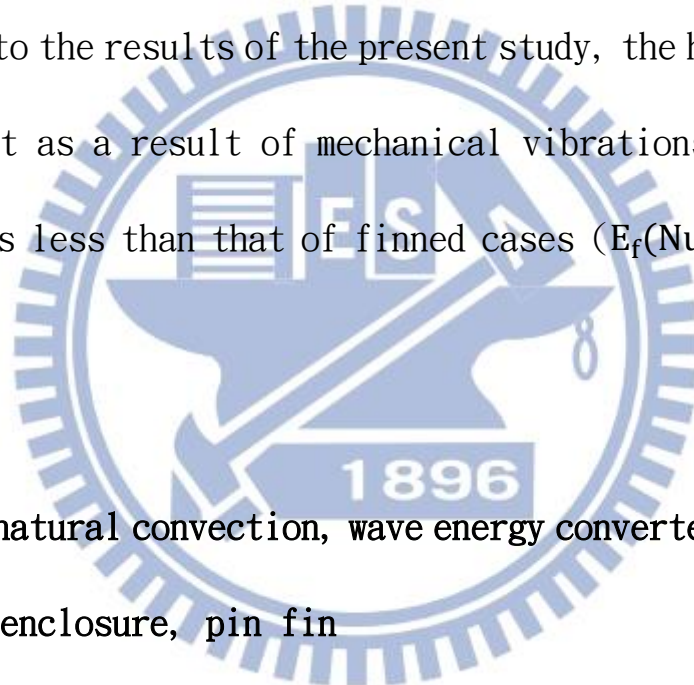
In the recent years, the development of the renewable energy industry in Taiwan has matured gradually. The prototype of the experiment in this study is a 20 kW class wave energy converter (WEC) from Industrial Technology Research Institute (ITRI). Because of large amount of electronic equipment in WEC chamber, the heat dissipation becomes an issue due to the sealed chamber.

This study aims to investigate the natural convection associated with mechanical vibrations and pin fins in a

cylindrical cavity with the heated surface facing upward. The mechanical vibration is produced by a stepper motor and an oscillation mechanism to simulate the operating condition of the WECs in the sea. The experimental parameters include different cavity height ($H=2.5\text{cm}$, 5cm), vibrational frequency ($f=1\text{Hz}$, 2Hz), and Rayleigh number ($Ra=5 \times 10^4 \sim 6 \times 10^5$).

According to the results of the present study, the heat transfer enhancement as a result of mechanical vibrations ($E_v(\text{Nu})$, $1.0 \sim 1.1$) is less than that of finned cases ($E_f(\text{Nu})$, $1.1 \sim 1.4$).

Keywords: natural convection, wave energy converter, vibration, enclosure, pin fin



誌謝

兩年的碩士生涯說快不快，說慢不慢，在交大的這兩年中，有歡笑也有淚水。但無論如何，在交大這個學術風氣鼎盛的環境下，我學到了不只是豐富的學術知識，而是更重要的做學問所需的嚴謹態度。我最感謝的，是我的指導老師 劉耀先教授，老師除了在實驗以及論文撰寫上給予相當多的建議，也在口頭報告的技巧上給我許多啟發，尤其感謝老師在我應徵台積電實習時幫忙寫推薦函，使我能提早接受職場磨練，也能把握拓展人脈的機會，獲益匪淺。至於在實驗的進行、機台的架設與軟體的模擬上，也要特別感謝元祥學長給我的諸多建議與幫忙，讓我能順利完成工研院計畫與學位論文。

另外冠甫、靖翔這些實驗室的同學與學弟，謝謝你們曾經幫助過我的一切，也要謝謝今年即將進入實驗室的乙軒學弟能接下我的工作，希望你們能夠延續實驗室的優良傳統。最後則是要感謝我的祖母，在我求學過程中無悔地提供經濟支援，讓我能順利完成大學及碩士學業，您從小將我撫養長大，沒有您就沒有今天的我，由衷的感謝您為我做的一切。

顥儒 謹致

2013/7 于風城交大

Contents

Chinese Abstract.....	I
English Abstract.....	III
Acknowledgement.....	V
Contents	VI
List of Tables.....	VII
List of Figures.....	VIII
Nomenclature.....	X
Chapter 1 Introduction.....	1
Chapter 2 Experimental Setup and Procedure.....	8
Chapter 3 Data Reduction.....	12
Chapter 4 Results and Discussion.....	17
Effect of fins.....	18
Effect of mechanical vibrations	21
Effect of enclosure height	23
Comparisons.....	25
Chapter 5 Conclusion.....	26
References	28

List of Tables

Table 1. Uncertainties in test parameters.....	43
Table 2. The $E_f Nu$ for stationary case ($f=0$)	44
Table 3. The $E_f Nu$ for vibrational case ($f=1\text{Hz}$)	44
Table 4. The $E_f Nu$ for vibrational case ($f=2\text{Hz}$)	45
Table 5. The $E_v Nu$ for smooth case	46
Table 6. The $E_v Nu$ for finned case	47
Table 7. The Nu increase due to increasing H for smooth case	48
Table 8. The Nu increase due to increasing H for finned case	49

List of Figures

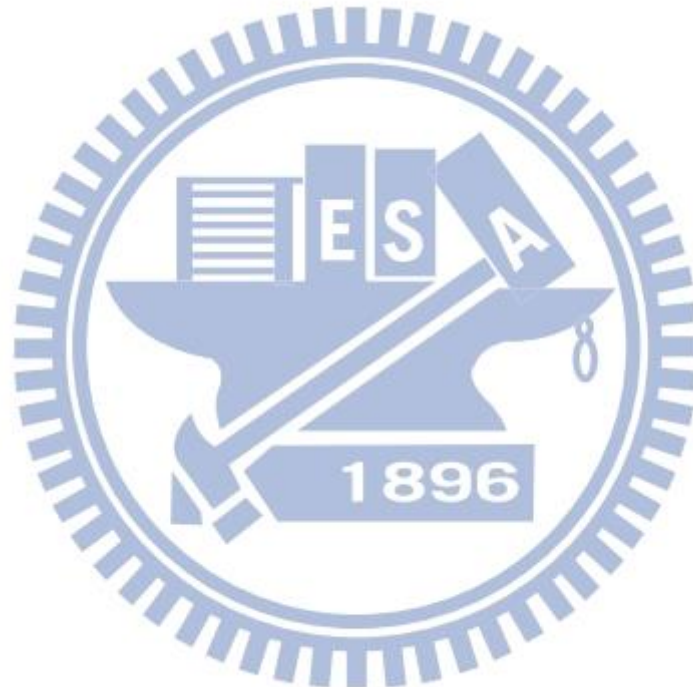
Figure 1. Experimental apparatus.....	33
Figure 2. Combination of test chamber and oscillation mechanism	33
Figure 3. NI-9213 device.....	34
Figure 4. Chiller.....	34
Figure 5. Test chamber cutaway view.....	35
Figure 6. Constants for equation (3.6).....	36
Figure 7. The comparison of Nu between theoretical and experimental results without fins and vibrations.....	36
Figure 8. Effect of fin installation on Nu without vibrations	37
Figure 9. Effect of fin installation on Nu with vibrations (f=1Hz)	37
Figure 10. Effect of fin installation on Nu with vibrations (f=2Hz)	38
Figure 11. The $E_f Nu$ in different H for (a) f=0 (b) f=1Hz (c) f=2Hz	39
Figure 12. Effect of mechanical vibrations on Nu with smooth base plate (H=5cm).....	40
Figure 13. Effect of mechanical vibrations on Nu with smooth base plate (H=2.5cm).....	40

Figure 14. Effect of mechanical vibrations on Nu with finned base plate (H=5cm)..... 41

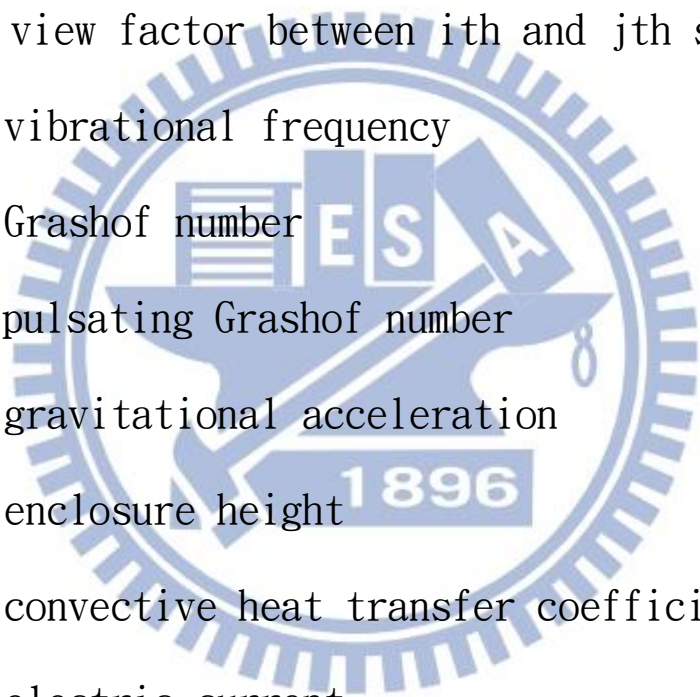
Figure 15. Effect of mechanical vibrations on Nu with finned base plate (H=2.5cm)..... 41

Figure 16. The E_vNu in different Grp with smooth base plate 42

Figure 17. The E_vNu in different Grp with finned base plate 42



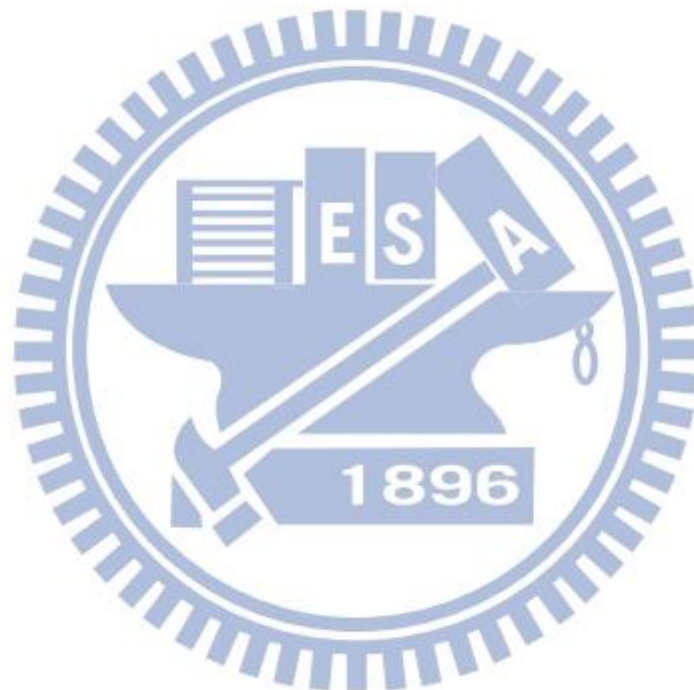
Nomenclature



A	base plate area
$E_f(Nu)$	increase of Nu due to fin installation
$E_v(Nu)$	increase of Nu due to mechanical vibrations
F_{ij}	view factor between i th and j th surface
f	vibrational frequency
Gr	Grashof number
Gr_p	pulsating Grashof number
g	gravitational acceleration
H	enclosure height
h	convective heat transfer coefficient
I	electric current
J	radiosity
k_a	thermal conductivity of acrylic wall
k_f	thermal conductivity of the fluid
k_w	thermal conductivity of Balsa wood
L	fin length

L_{ch}	characteristic length
m	constant for equation (3.6)
Nu	Nusselt number of base plate
Nu_{film}	Nusselt number determined by T_{film}
P	power input of the heater
Pr	Prandtl number of the fluid
Q_{con}	conductive heat loss
Q_{conv}	convective heat transfer rate
Q_{rad}	radiative heat loss
R	resistance of the heater
Ra	Rayleigh number of the fluid
S	fin spacing
T_c	temperature of the cold plate
T_{film}	film temperature
T_w	temperature of base plate
ΔT	temperature difference ($T_w - T_c$)
α	thermal diffusivity
β	thermal expansion coefficient
ε	emissivity

σ Stefan-Boltzman coefficient
 ν kinematic viscosity



Chapter 1

Introduction

Natural convection heat transfer in an enclosure is usually an issue for many applications such as electronic equipment, low temperature logistics and oil cargos in a ship tank. Earlier relevant studies mostly concentrated on the configuration of an enclosure of which side is an energy source. For applications mentioned above, the bottom side is often a heat transfer area and is different from the previous study. This paper, however, is devoted to investigate the natural convection heat transfer influenced by the similar disturbance that could cause flow pattern variation, like mechanical oscillation of the wall, cavity height and the imparting of heat dissipation module. In heat transfer applications, pin fins are often utilized due to low manufacturing cost and high heat transfer enhancement. Moreover, the most common design of pin fin configuration is in-line and is used in this study.

Natural convection in an enclosure has various

characteristics with different aspect ratio due to convection flow pattern change. Bejan [1] and Bejan and Tien [2] studied the influence of height to length ratio on natural convection in a cavity with two opposite side walls with different end temperatures. They showed that the height to length ratio of the cavity causes three regimes of natural convection heat transfer based on the change of flow pattern and resistance to heat transfer. They are : (1) $Ra \rightarrow 0$ regime, (2) intermediate regime and (3) boundary layer regime. The heat transfer rate and mechanism depends on the height to length ratio and the Rayleigh number of the fluid between these two isothermal boundaries. After the preliminary study, Kimura and Bejan [3] carried out further investigation of natural convection heat transfer in a shallow enclosure at boundary layer regime (for high Rayleigh number). According to this investigation, the boundary layer thickness of the vertical constant heat flux wall is constant and results in linear conversion of temperature in constant heat flux wall and fluid core region. Ganguli et al. [4] conducted an experimental study of

optimization of cooking device insulation. The effects of cooking device width (convection cell development length) were studied with different height. The heat transfer coefficient increases with increasing the width of the cavity as a result of expansion, breaking of boundary layer near the walls, and multiple convection cells development due to fluid instability.

The interaction between convection and oscillation of enclosure has been investigated for years. Fand [5] and Richardson [6] proposed some explanations for this interaction in the early years. Mathematical model of this interaction is a complicated derivation rather than the combination of stationary and vibrations merely. The energy of vibrations induces oscillating vortex near the boundary walls and increase the heat transfer rate between wall and fluid medium. At higher turbulent intensity, the fluctuation and velocity gradient of fluid give rise to acoustic streaming. For transverse and vertical vibrations, the oscillation direction and gravitational force influences the boundary layer near the wall.

Detailed numerical examination of natural convection affected by mechanical vibrations and gravitation was conducted by Fu and Shieh [7-8]. The study showed that the oscillation could enhance the heat transfer rate due to additional fluid circulation caused by oscillation. They also concluded that higher oscillation frequency could be a vortex generator. This result was once more experimentally confirmed by Kim et al. [9]. To verify the agreement between numerical and experimental results, this study also introduced a motor mechanism to simulate the oscillation motion and had great agreement with former numerical result. Similar experimental or numerical investigations [10-15] were conducted with diverse parameters and also have good agreement with literatures [5-6].

Pin fin heat sink is a versatile module of heat dissipation for various engineering systems. Generally speaking, the heat transfer rate on a finned surface increases with increasing the number of fins due to increase of heat dissipation area. For optimization of heat dissipation, it is necessary to study and confirm the optimum fin configurations. Sahray et al. [16]

performed an investigation of the influence of fin population density on the flow field on a finned horizontal base. Inada et al. [17] conducted a work experimentally on a finned base enclosure heated from below to investigate and visualize the fluid flow characteristics with different fin insertion interval. These studies reported that the variation in heat transfer rate affected by certain number of fins is larger than that of affected by heat dissipation area. The limitation of fin spacing results in inactive convection cells between fins and decreases the heat transfer rate. In addition, the fin optimal configuration is independent of the temperature difference between fin and ambient fluid medium. Some surveys [18-19] also presented similar and more detailed consequence about the effect of fin to enclosure height ratio and fin spacing on heat transfer rate of a finned isothermal plate in a horizontal fluid layer. These studies showed that the high fin length to enclosure ratio improve the fin effectiveness as a result of increasing of heat dissipation area and stronger, distinguishable convection cells in the space between fins.

Also, the fin effectiveness decreases with increasing Rayleigh number due to increasing flow resistance induced by increase of fin length. Bocu and Altac [20] studied the natural convection in an enclosure with finned and heated side wall opposite to a cold one. They found the same results as mentioned above.

A numerical study was conducted to investigate the natural convection heat transfer from a number of horizontal vibrating and isothermal cylindrical projections by Shokouhmand et al. [21]. The fluid thermal boundary layer near the projections breaks and is disturbed by vibrations. Thus, the local convection heat transfer increases due to enhancement of fluid flow circulation closed to the heated projections' surface. Nag and Bhattacharya [22] conducted an experimental investigation to combine the free convection around the long vertical cuboid fin arrays with mechanical vibrations. This study showed that a threshold value of vibrational intensity which is the product of oscillation amplitude and frequency. There is no obvious increase of heat transfer rate from those

attached fins until the vibrational intensity reaches a certain value. That is, the boundary layer near the fins does not become chaotic up to a certain vibrational intensity. However, this study also has a conclusion that the heat transfer decreases due to increasing in fin length and is conflicting with the results of literature [18].

As mentioned previously, there are literatures which investigate and optimize the fin configurations to improve heat transfer. To the author's knowledge, however, there are no investigations of natural convection in an enclosure with finned heated plate coupled with mechanical vibrations. Therefore, this study focuses on the investigation of relevance between internal natural convection, cylindrical pin fins, and mechanical vibrations ($f=1\text{Hz}$, 2Hz).

Chapter 2

Experimental Setup and Procedure

The apparatus in this study contain three main parts, one is stepper motor and transmission mechanism, another is test chamber, the other is thermocouple data acquisition system. The entire experimental apparatus diagram is shown in Fig. 1-2.

The stepper motor is manufactured by SANYO DENKI (1.8 degrees step angle, two phase, the maximum torque is 70 kg-cm). It connects to a controller manufactured by Parker via RS232 port to a personal computer. The transmission mechanism is composed of linear guideway, linear slider, metal disk and connective rod. The linear guideway sets can ensure that the cavity only have one-dimensional vertical motion. Metal disk and connective rod connect the cavity and stepper motor.

To conduct precise temperature measurement, OMEGA T-type thermocouple and thermocouple data acquisition device (NI-9213) are adopted as shown in Fig. 3. The thermocouple is composed of copper and copper-nickel metal filament. The two metal

filaments were welded in endpoint to form a closed electrical loop and to conduct temperature measurement by voltage difference between the two metal filaments. The voltage difference causes a current through the loop and that can be transformed to a temperature difference compared to a reference point, which is known as thermoelectric effect. Because of the measurement errors, the thermocouple should be calibrated before using. The thermocouple measurement error was found to be about $\pm 0.2^{\circ}\text{C}$. The input signal of thermocouple is analog so that it must be transformed to digital signal, and interpreted by LabVIEW Signal Express program.

The test chamber is an annular acrylic wall with inner diameter of 15 cm, outer diameter of 17.2 cm, and height of 10.7 cm. Balsa wood is machined for the bottom side of the enclosure, and these plates served as heat insulation layers to reduce the heat loss. The outside acrylic wall is wrapped in ceramic fiber insulating blanket to prevent heat loss through the side walls. A polyimide film (kapton) flexible heater (25 W) which is controlled by a laboratory DC power supply was used to heat the

copper plate. The thickness of the copper plate is 1mm in order to reduce the heat loss through acrylic wall. The heater was fixed on the copper plate by thermal conductive grease and high temperature silicon. An aluminum cold water container was placed at the top of the acrylic wall as a low temperature plate for the natural convection. The cold water is provided by an air cooled chiller as shown in Fig. 4 and the water is pumped into the aluminum container to control the temperature. Two thermocouples were attached to the backside of the copper plate. In order to calculate the conductive heat loss through acrylic wall and Balsa wood insulation layer, there were seven thermocouples attached to the acrylic wall and three thermocouples attached to the bottom side of Balsa wood insulation layer. For finned base plate case, copper cylindrical fins were attached to the base plate by super glue and were placed as in-line arrangement. The diameter of the fins is 1 cm and the height is 1 cm. The increase of heat transfer area due to fin insertion is about 30.1% of the original heat transfer area. Locations of the thermocouples in the test

chamber are plotted in Fig. 5.

After the preparation of the test section, the power supply was switched on to provide electrical power to the heater.

Rayleigh numbers are varied by changing the surface temperature and the enclosure height. The air cooled chiller was activated

to pump and cool the water flows through the aluminum container above acrylic wall. When steady state condition was achieved,

the thermocouple data acquisition device captured and read the data from thermocouples. The steady state condition was reached

when the temperature of copper base plate fluctuation is less than $\pm 0.3^{\circ}\text{C}$ within 30 min. Vibrational condition was performed

after the recording of stationary condition result. The personal computer transmitted the text file in which the motor

controlling orders were written to the stepper motor controller.

In vibrational case, the steady state condition is the same as stationary case. For both smooth and finned cases, the

experimental procedures and conditions were the same.

Chapter 3

Data Reduction

In convection heat transfer, the Rayleigh number is the principal dimensionless parameter which determines whether the convection is turbulent or laminar. The Rayleigh number is defined as:

$$Ra = \frac{g \cdot \beta \cdot (T_w - T_c) \cdot L_{ch}^3}{\nu \cdot \alpha} = GrPr \quad (3.1)$$

where g is gravitational acceleration constant, β is volumetric expansion coefficient, ν is kinematic viscosity, α is thermal diffusivity, T_w is surface temperature, T_c is the cold plate temperature, L_{ch} is characteristic length, Gr is Grashof number, and Pr is Prandtl number. The fluid properties are determined by film temperature which is defined as:

$$T_{film} = \frac{T_w + T_c}{2} \quad (3.2)$$

In all natural convection empirical correlations, it is necessary to calculate Rayleigh number of the fluid. The Nusselt number is defined as:

$$Nu = \frac{\text{conduction thermal resistance}}{\text{convection thermal resistance}} = \frac{hL_{ch}}{k_f} \quad (3.3)$$

where h is heat transfer coefficient, k_f is thermal conductivity of the fluid. The power consuming by heater inside the cavity is evaluated by electrical power formula which is express as:

$$P = I^2 \times R \quad (3.4)$$

where P is the electrical power consumed by heater, I is the current input to the heater, and R is the linear resistance of the heater. The convection coefficient can be calculated from basic convection formula:

$$Q_{conv} = h \times A \times \Delta T \quad (3.5)$$

where Q_{conv} is convective heat transfer rate, h is heat transfer coefficient, A is the surface area, ΔT is the temperature difference between the hot surface and the cold plate above acrylic wall. Then the Nusselt number can be calculated by equation (3.3).

For various geometric situations, there is an empirical equation for natural convection heat transfer:

$$Nu_{film} = C(Gr_{film}Pr_{film})^m \quad (3.6)$$

where C and m are constants as shown in Fig. 6 and the subscript

film indicates that the dimensionless parameter should be determined by equation (3.2). In this study, the parameters C and m were chosen to be 0.54 and 0.25 respectively.

In the experiment of this study, the conduction and radiation heat transfer are redundant that result in experimental inaccuracy. To obtain precise information, the redundancy, namely, the heat loss, must be excluded from the study. Because P is equal to the total heat transfer from the heater according to energy conservation, the convective heat transfer Q_{conv} can be given by:

$$Q_{conv} = P - Q_{con} - Q_{rad} \quad (3.7)$$

where Q_{con} is conduction heat loss through acrylic wall and Balsa wood insulation layer, Q_{rad} is radiative heat loss of the emission and reflection from internal acrylic wall and copper plate to the aluminum container surface. Q_{con} can be expressed as:

$$Q_{con} = k_w \frac{T_w - T_b}{t_w} + k_a \frac{T_i - T_e}{t_a} \quad (3.8)$$

where k_w is thermal conductivity of Balsa wood, k_a is the thermal conductivity of acrylic wall, t_w is the thickness of

Balsa wood insulation layer, t_a is the thickness of acrylic wall, T_b is the temperature of bottom side of Balsa wood insulation layer, T_i is the temperature of internal side of acrylic wall, T_e is the temperature of external side of acrylic wall. The net radiative heat transfer between two non-black surface is [23]:

$$Q_{\text{net}} = \frac{\sigma(T_1^4 - T_2^4)}{(1-\epsilon_1)/\epsilon_1 A_1 + 1/A_1 F_{12} + (1-\epsilon_2)/\epsilon_2 A_2} \quad (3.9)$$

where ϵ is the emissivity of non-black surface, F_{12} is the view factor between the two surfaces, A is the surface area. The radiation heat loss can be calculated as follows [18]:

$$Q_{\text{rad}} = \epsilon_c A_c (\sigma T_c^4 - G_c) \quad (3.10)$$

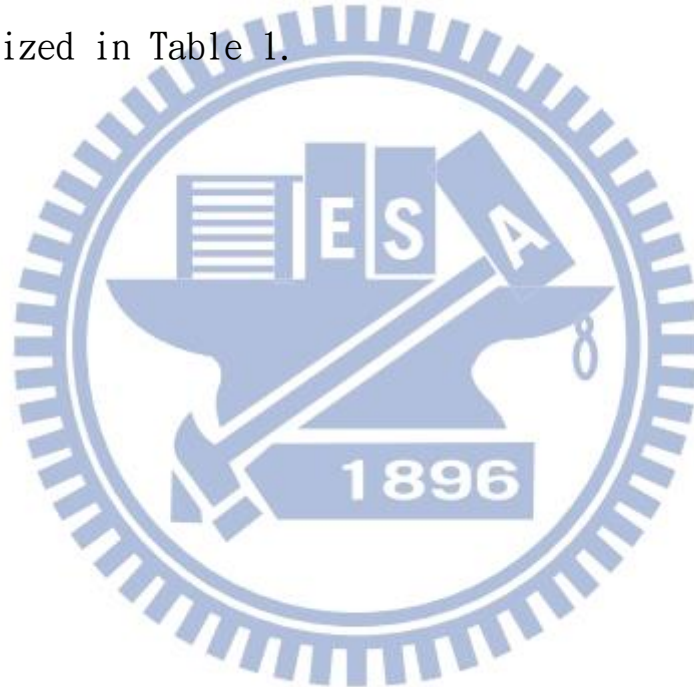
where the subscript c represents the aluminum container, G_c is the net irradiation on the cold plate above acrylic wall and G_c is given by:

$$G_c = \sum_{j=1}^2 F_{cj} J_j \quad (3.11)$$

where the subscript j represents the internal surface of acrylic wall and Balsa wood insulation layer, F_{cj} is the view factor between aluminum container surface and j th internal surface, J_j is radiosity of the j th internal surface given by:

$$J_j = \epsilon_j \sigma T_j^4 + (1 - \epsilon_j) \sum_{j=1}^2 F_{ji} J_i \quad (3.12)$$

In order to obtain J_j , a linear system of J_j variables are solved by Engineering Equation Solver (EES) software. The view factor F_{ji} is given by reference [25]. The heat loss is 8%–15% of the total input power. The uncertainties of the test parameters are based on the calculation of literature [26] and are summarized in Table 1.



Chapter 4

Results and Discussion

In this study, experimental investigation had been conducted to examine the effects of mechanical vibrations and fin installation on the natural convection heat transfer in a cylindrical enclosure. Different configurations were introduced in the investigation. They were: (1) absence and presence of fins, (2) with and without mechanical vibrations and (3) different enclosure height.

The comparison between theoretical and measured Nusselt number (Nu) of heated base plate without fins and mechanical vibrations is shown in Fig.7 for different enclosure height. The empirical correlation is based on equation (3.6) for upper surface of heated plates and the deviation is within 10%–22% from the experimental results.

Effect of fins

Fig. 8-10 depict the influence of fin on Nusselt number distribution. A dimensionless parameter Gr_p for vibrational cases was adopted [27]. Gr_p is defined as:

$$Gr_p = \frac{\omega^2 a \beta (T_w - T_c) H^3}{\nu^2} \quad (4.1)$$

where ω is angular velocity of rotating disc driven by stepper motor, a is vibrational amplitude. Gr_p represents the ratio of buoyancy force induced by mechanical oscillation to viscous force.

For any Ra and Gr_p , the Nu of finned plate is larger than smooth case. In stationary and vibrational cases without fins, the Nu increases with increasing Ra or Gr_p continuously. In those cases with fins, however, the increase of Nu with Ra or Gr_p is small compared to those of the cases without fins, and decreases with increasing Ra or Gr_p occasionally. Therefore, the heat transfer rate enhancement due to fin attachment ($E_f(Nu)$) decreases with increasing Ra or Gr_p . In natural convection, the Ra is dominant because the flow circulation is

induced by spontaneous driven force (buoyancy force). When Ra is high enough, the other influential factors like heat transfer area become minor and relatively unimportant. Therefore, the effectiveness of fin installation is smaller in higher Ra or Gr_p .

The fin insertion influences flow characteristics inside the enclosure. According to literature [17-19], the fin insertion enhances the probability of split of convection cells and increases the heat transfer area. The convection cells are almost square and the same size in bare base plate configuration. The fin insertion increases the number of convection cells resulting in enhancement of heat transfer, and narrows down the convection cell development resulting in reduction of heat transfer due to decreasing of flow intensity. Moreover, increasing the heat transfer area induces further obstruction for flow circulation due to viscous effect along the fin wall. The fin insertion increases the heat transfer generally due to increasing heat transfer area, however, the heat transfer may decrease under certain fin configurations like dense fin

spacing due to the results of [18].

In the present study, the fin configurations were:

$S/H = 0.4, 0.8$ and $L/H = 0.2, 0.4$ where S is fin spacing, L is fin length, H is enclosure height. The fin spacing to enclosure height ratio is smaller or equal to the experimental configurations of literature [18] which states that $S/H = 0.8$ results in decreasing Nu compared to larger S/H . For $S/H = 0.8$ and $L/H = 0.4$, the deviation of Nu of the base plate from the results of [18] at the same Ra is 8%-12% approximately. For smaller L/H , the reduced space between fin tip and top wall of enclosure results in increase of temperature gradient according to the results of [19]. More distinct convection cells appear in the space between fins at larger L/H . Fig. 11 shows that the $E_f(Nu)$ at smaller L/H is always greater than the cases at larger L/H in all stationary and vibrational cases. It is probably as a result of insufficient space where convection cells develop due to decreasing the enclosure height. The heat transfer enhancement due to more distinct convection cells cannot overcome the weakening of heat

transfer due to decreasing the space for convection cells development. The $E_f(Nu)$ is listed in Table 2-4.

Effect of mechanical vibrations

Fig. 12-15 show the enhancement of heat transfer due to mechanical vibrations. In the cases without fins, the Nu of base plate increases at any Gr_p compared to stationary cases. These figures also show that the Nu increase tendency at lower H appears to be contrary to the case which is at larger H in all vibrational cases. It is probably due to the space for convection cells to develop. At smaller H, the space for convection cells development is insufficient for convection cells development due to superimposing mechanical vibrations. Thus the increase of heat transfer due to mechanical vibrations is indistinct with increasing Gr_p under the same vibrational conditions. Contrarily, at larger H, there is enough space to develop convection cells induced by mechanical vibrations. Thus the heat transfer increase due to mechanical vibrations

is relatively significant at larger H . For finned base plate cases, the increase of heat transfer appears to be irregular. To the author's knowledge and the explanations of literature [5-6], the fluctuating velocity exists in the natural convection flow due to mechanical vibrations and the rugged finned base plate surface also disturb the propagation of fluid momentum. Moreover, the velocity gradient is also induced because the base plate diameter was long compared to the vibration amplitude. The figure also shows that the heat transfer did not increase significantly in all vibrational cases. According to the results of [22], the Nusselt number did not change significantly upto a threshold value of vibrational intensity (af). The Nusselt number increases in large amplitude abruptly when the af is high enough to disturb the boundary layer and the fluid tends to be turbulent. According to the results of [8-9], the heat transfer rate increases significantly and abruptly in a certain vibration frequency which is called the resonant frequency. At the resonant frequency, the intensity of the convection cell rotating can

be enhanced due to increasing the intensity of stream function. In the present study, the af was probably not high enough to disturb the boundary layer and keep the fluid in laminar, and the vibration frequency did not reach the resonant condition. Fig. 16-17 shows the heat transfer rate enhancement tendency due to mechanical vibrations ($E_v(Nu)$). The $E_v(Nu)$ was found to be not significant (maximum of 1.07) due to the reasons as mentioned above. To sum up, the crucial factor of increasing heat transfer for mechanical vibrations is the boundary layer transition for laminar to turbulent. The vibration amplitude to the characteristic length of object is also necessary to be considered in this sort of study. The $E_v(Nu)$ is listed in Table 5-6.

Effect of enclosure height

The natural convection in an enclosure heated from below begins to form multiple convection cells which is known as

Bénard cells when the Ra exceeds a certain value. According to (3.1), the influence of characteristic length on Ra is greater than that of temperature difference. At the same temperature difference and vibrational conditions, the increase of Nu due to increasing enclosure height is about 79%-116% which is listed in Table 7-8. The higher enclosure height tends to not only induce higher buoyancy force due to enough space for convection cells to develop, but also enhance the probability of vortex forming, resulting in larger heat transfer rate. Also, the increase of Nusselt number at higher enclosure height with finned base plate is larger than those of smooth plate in most cases. The fin installation increases the heat transfer area. Although increasing heat transfer area raises the viscous effect, the higher buoyancy effect due to increased enclosure height overcomes the viscous effect and the heat transfer is raised due to increasing heat transfer area.

Comparisons

In all cases, the heat transfer enhancement as a result of fin installation exceeds the one as a result of superimposing mechanical vibrations. This can be attributed to which the energy of vibrations can be consumed by viscous effect. The energy of vibrations must propagate through the interface between fluid layer and solid wall. The vibrational energy is transferred to the fluid medium incompletely. Thus the flow circulation is not intense as expected. According to the experimental results of this study, the change of heat transfer due to increasing heat transfer area is higher than the cases due to superimposing mechanical vibrations.

Chapter 5

Conclusion

Natural convection in a cylindrical horizontal narrow enclosure with finned heated base plate had been investigated experimentally. The influence of mechanical vibrations and enclosure height on natural convection heat transfer was studied for three cases of temperature difference ($T_w - T_c$). For fin installation cases, the fin insertion increases the heat transfer area and the probability of convection cell splitting. Although increasing heat transfer area enhance viscous effect resulting in reducing flow intensity, the heat transfer rate was still improved under the conditions conducted in this study. Increasing Ra reduces $E_f(Nu)$ due to the domination of Ra in natural convection. The $E_f(Nu)$ also decreases with decreasing L/H .

For mechanical vibrations effect, the heat transfer enhancement due to mechanical vibrations at any Gr_p was not significant in the present study. Moreover, the increase of

Nusselt number due to mechanical vibrations increases with increasing Gr_p at higher enclosure height and it is contrary to the cases at lower enclosure height.

For changing enclosure height, the higher enclosure height inducing larger buoyance effect due to increasing Ra was confirmed experimentally. The heat transfer enhancement at higher enclosure height with finned base plate was greater than those of bare base plate and the maximum heat transfer enhancement due to increasing enclosure height (2.5cm \rightarrow 5cm) was found to be about 79%-116%. Under any temperature and vibration conditions, the increase of Nusselt number due to increasing enclosure height was greater than the cases due to fin insertion and mechanical vibrations.

The $E_f(Nu)$ was greater than $E_v(Nu)$ in all temperature and vibration cases. With smooth base plate, the $E_v(Nu)$ was always greater than one at any Gr_p , however, the $E_v(Nu)$ development was found to become instable with finned base plate and is less than one at certain Gr_p .

References

- [1] A. Bejan, Convection heat transfer 2nd ed., Wiley, New York, 1995.
- [2] A. Bejan, C.L. Tien, “Laminar natural convection heat transfer in a horizontal cavity with different end temperatures” , J. Heat Tran., 100, pp. 641-647, 1978.
- [3] S. Kimura, A. Bejan, “The boundary layer natural convection regime in a rectangular cavity with uniform heat flux from the side” , J. Heat Tran., 106, pp. 98-103, 1984.
- [4] A.A. Ganguli, A.S. Gudekar, A.B. Pandit, J.B. Joshi, “A novel method to improve the efficiency of a cooking device via thermal insulation” , Can. J. Chem. Eng., 90, pp. 1212-1223, 2012.
- [5] R.M. Fand, “Mechanism of interaction between vibrations and heat transfer” , J. Acoust. Soc. Am., 34, pp. 1887-1894, 1962.
- [6] P.D. Richardson, “Effects of sound and vibrations on heat transfer” , Appl. Mech. Rev., 20, pp. 201-211, 1967.

- [7] W.S. Fu, W.J. Shieh, “Transient thermal convection in an enclosure induced simultaneously by gravity and vibration” , Int. J. Heat Mass Tran., 36, pp. 437-452, 1993.
- [8] W.S. Fu, W.J. Shieh, “A study of thermal convection in an enclosure induced simultaneously by gravity and vibration” , Int. J. Heat Mass Tran., 35, pp. 1695-1710, 1992.
- [9] S.K. Kim, S.Y. Kim, Y.D. Choi, “Resonance of natural convection in a side heated enclosure with a mechanically oscillation bottom wall” , Int. J. Heat Mass Tran., 45, pp. 3155-3162, 2002.
- [10] V.D. Blankenship, J.A. Clark, “Effects of oscillation on free convection from a vertical finite plate” , J. Heat Tran., 86, pp. 149-158, 1964.
- [11] V.D. Blankenship, J.A. Clark, “Experimental effects of transverse oscillations on free convection of a vertical, finite plate” , J. Heat Tran., 86, pp. 159-165, 1964.
- [12] R.E. Forbes, C.T. Carley, C.J. Bell, “Vibration effects on convective heat transfer in enclosures” , J.

Heat Tran., 92, pp. 429–438, 1970.

- [13] A. S. Dawood, B. L. Manocha, S. M. J. Ali, “The effect of vertical vibrations on natural convection heat transfer from a horizontal cylinder” , Int. J. Heat Mass Tran., 24, pp. 491–496, 1981.
- [14] S. Akagi, K. Uchida, “Fluid motion and heat transfer of a high-viscosity fluid in a rectangular tank on a ship with oscillation motion” , J. Heat Tran., 109, pp. 635–641, 1987.
- [15] I. A. Babushkin, V. A. Demin, “On vibration-convective flows in a Hele-Shaw cell” , J. Eng. Phys. Thermophys., 81, pp. 739–747, 2008.
- [16] D. Sahray, H. Shmueli, G. Ziskind, R. Letan, “Study and optimization of horizontal-base pin-fin heat sinks in natural convection and radiation” , J. Heat Tran., 132, pp. 012503–13, 2010.
- [17] S. Inada, T. Taguchi, W. J. Yang, “Effects of vertical fins on local heat transfer performance in a horizontal fluid layer” , Int. J. Heat Mass Tran., 42, pp. 2897–2903,

1999.

- [18] S.A. Nada, “Natural convection heat transfer in horizontal and vertical closed narrow enclosures with heated rectangular finned base plate” , Int. J. Heat Mass Tran., 50, pp. 667–679, 2007.
- [19] E. Arquis, M. Rady, “Study of natural convection heat transfer in a finned horizontal fluid layer” , Int. J. Therm. Sci., 44, 43–52, 2005.
- [20] Z. Bocu, Z. Altac, “Laminar natural convection heat transfer and air flow in three-dimensional rectangular enclosures with pin arrays attached to hot wall” , Appl. Therm. Eng., 31, pp. 3189–3195, 2011.
- [21] H. Shokouhmand, S.M.A. Noori Rahim Abadi, A. Jafari, “The effect of the horizontal vibrations on natural heat transfer from an isothermal array of cylinders” , Int. J. Mech. Mater. Des., 7, pp. 313–326, 2011.
- [22] P.K. Nag, A. Bhattacharya, “Effect of vibration on natural convection heat transfer from vertical fin arrays” , Lett. Heat Mass Tran., 9, pp. 487–498, 1982.

- [23] J.P. Holman, Heat transfer 10th ed., McGraw-Hill, Boston, 2010.
- [24] F.P. Incropera, D.P. DeWitt, T.L. Bergman, A.S. Lavine, Fundamentals of heat and mass transfer 6th ed., Wiley, New York, 2007.
- [25] M.F. Modest, Radiative heat transfer, McGraw-Hill, Boston, 1993.
- [26] R.J. Moffat, “Using uncertainty analysis in the planning of an experiment” , J. Fluids Eng., 107, pp. 173-178, 1985.
- [27] S.W. Chang, L.M. Su, W.D. Morris, T.M. Liou, “Heat transfer in a smooth-walled reciprocating anti-gravity open thermosyphon” , Int. J. Therm. Sci., 42, pp. 1089-1103, 2003.

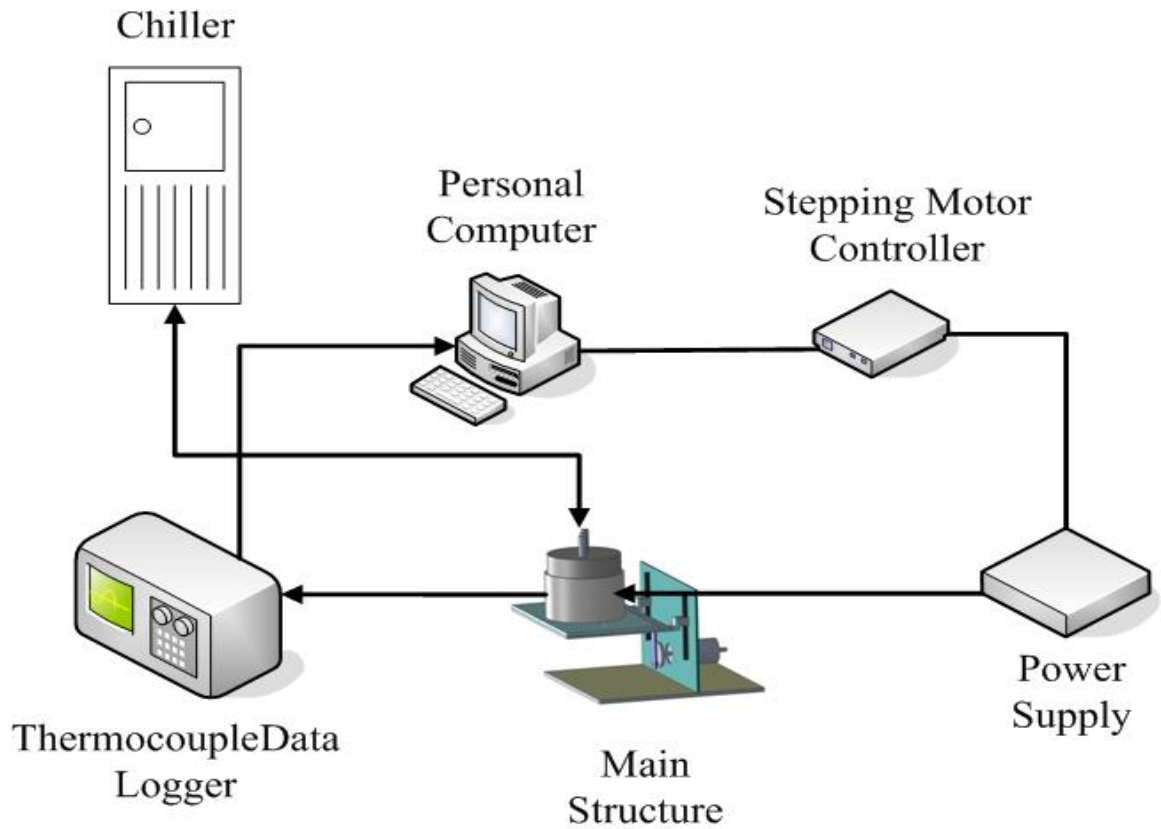


Figure 1. Experimental apparatus

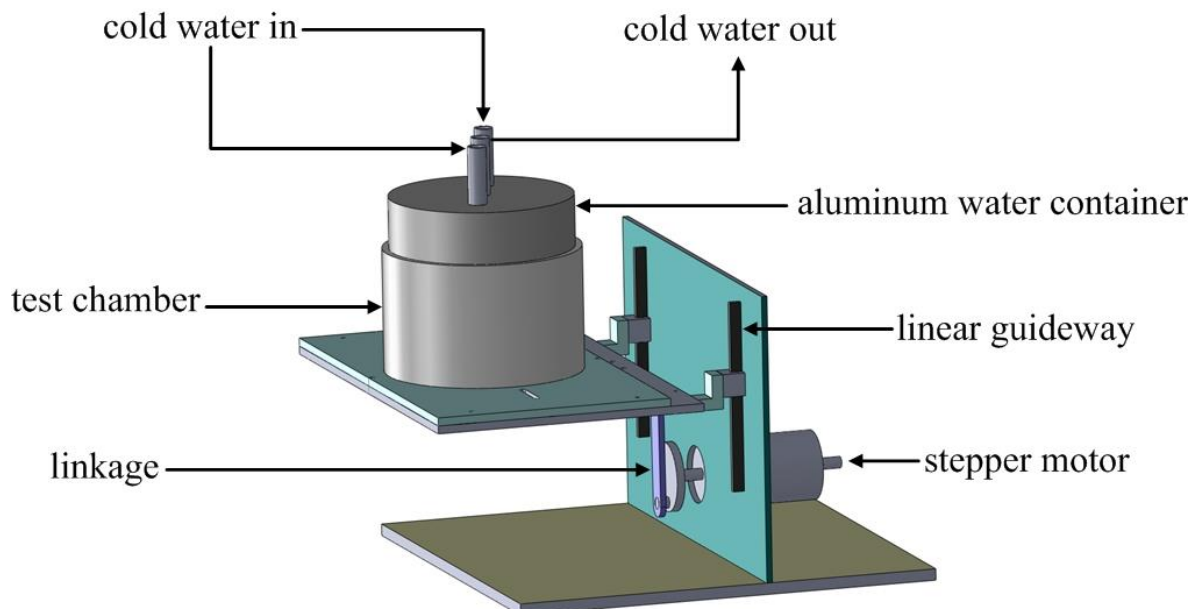


Figure 2. Combination of test chamber and oscillation mechanism

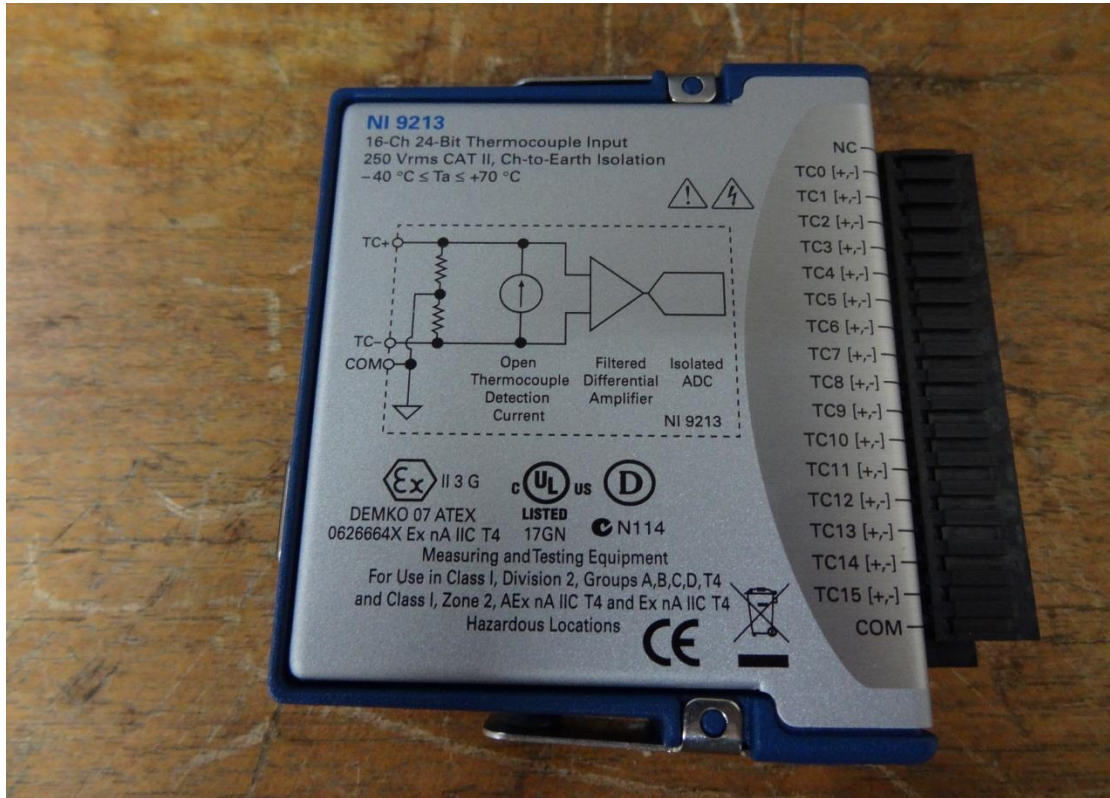


Figure 3. NI-9213 device



Figure 4. Chiller

- a. aluminum water container
- b. copper fin
- c. acrylic wall
- d. Balsa wood insulation layer
- e. heater
- f. copper plate
- g. thermocouple junction

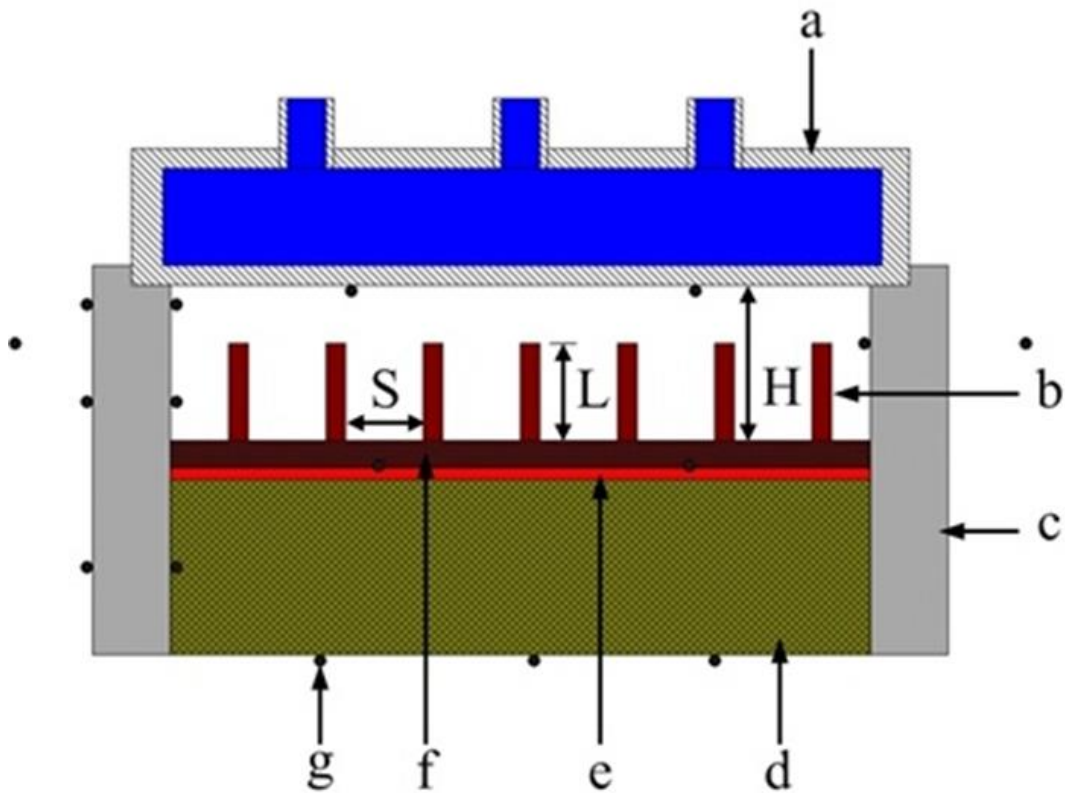


Figure 5. Test chamber cutaway view

Table 7.1 Constants for Equation 7.5 for isothermal surfaces

Geometry	Ra	c	m
Vertical planes and cylinders	10^{-1} - 10^4	use Figure 7.4	use Figure 7.4
	10^4 - 10^9	0.59	0.25
	10^9 - 10^{13}	0.1	1/3
Horizontal cylinder	0 - 10^{-5}	0.4	0
	10^{-5} - 10^4	use Figure 7.5	use Figure 7.5
	10^4 - 10^9	0.53	0.25
	10^9 - 10^{12}	0.13	1/3
	10^{10} - 10^{-2}	0.675	0.058
	10^{-2} - 10^2	1.02	0.148
	10^2 - 10^4	0.85	0.188
	10^4 - 10^7	0.48	0.25
10^7 - 10^{12}	0.125	1/3	
Upper surface of heated plates or lower surface of cooled plates	2×10^4 - 8×10^6	0.54	0.25
Upper surface of heated plates or lower surface of cooled plates	8×10^6 - 8×10^{11}	0.15	1/3
Lower surface of heated plates or upper surface of cooled plates	10^5 - 10^{11}	0.27	0.25
Vertical cylinder, height = diameter Characteristic length = diameter	10^4 - 10^6	0.775	0.21
Irregular solids Characteristic length = distance Of fluid particle travels in boundary layer	10^4 - 10^9	0.52	0.25

Figure 6. Constants for equation (3.6) [24]

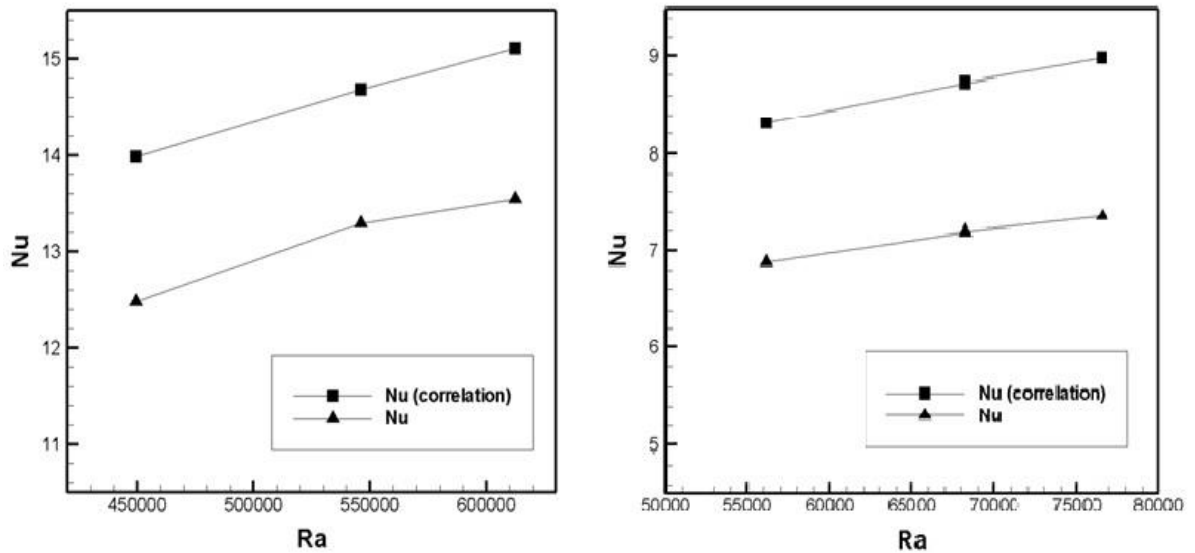


Figure 7. The comparison of Nu between theoretical and experimental results without fins and vibrations

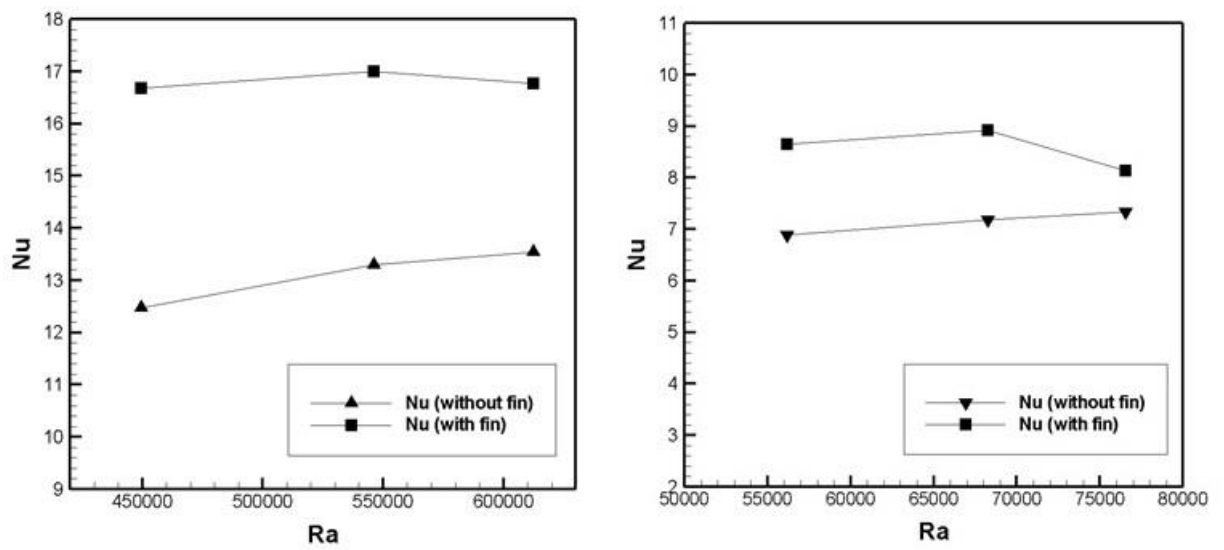


Figure 8. Effect of fin installation on Nu without vibrations

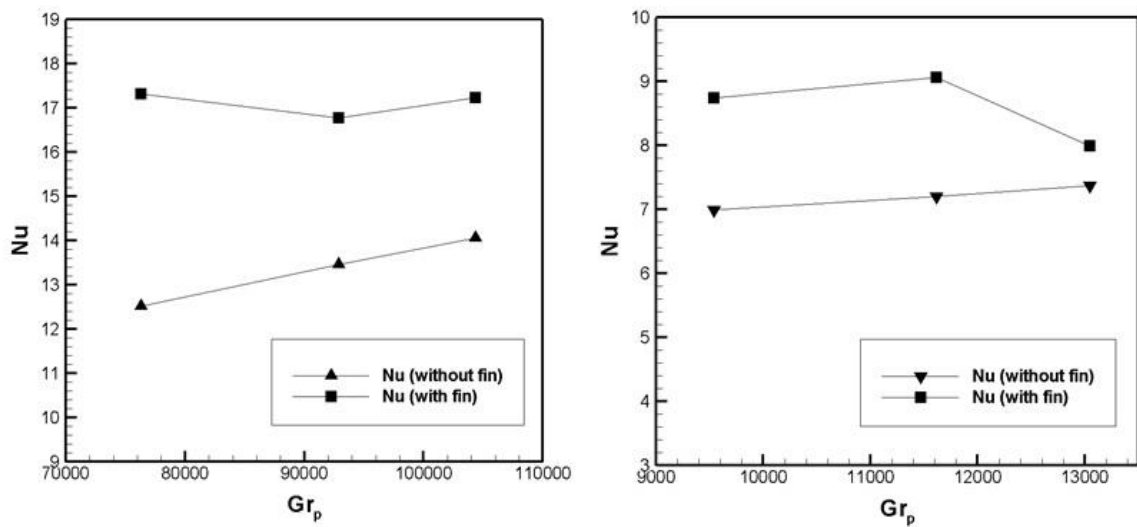


Figure 9. Effect of fin installation on Nu with vibrations ($f=1\text{Hz}$)

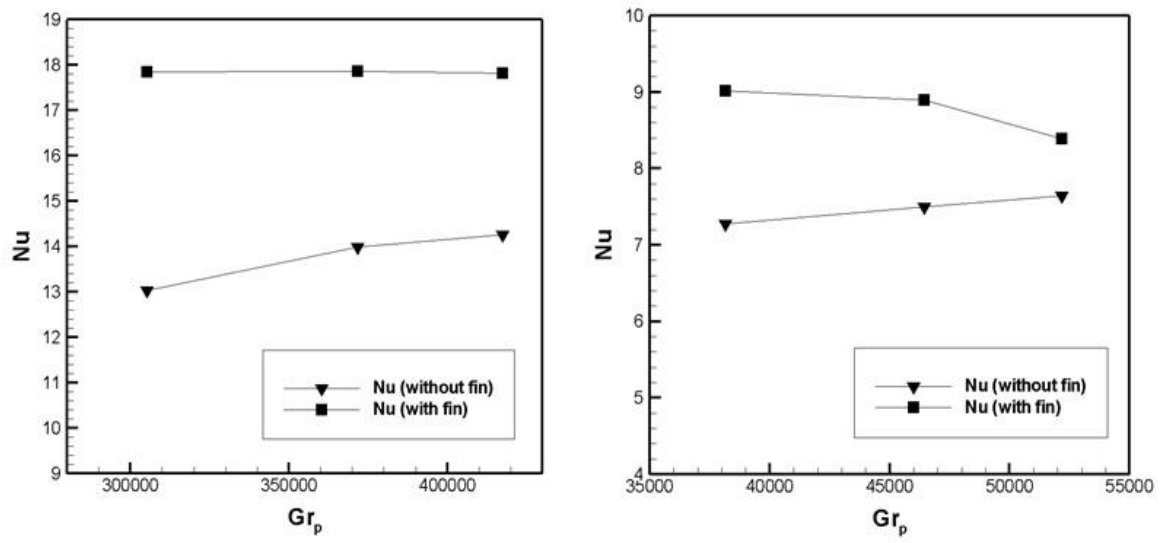
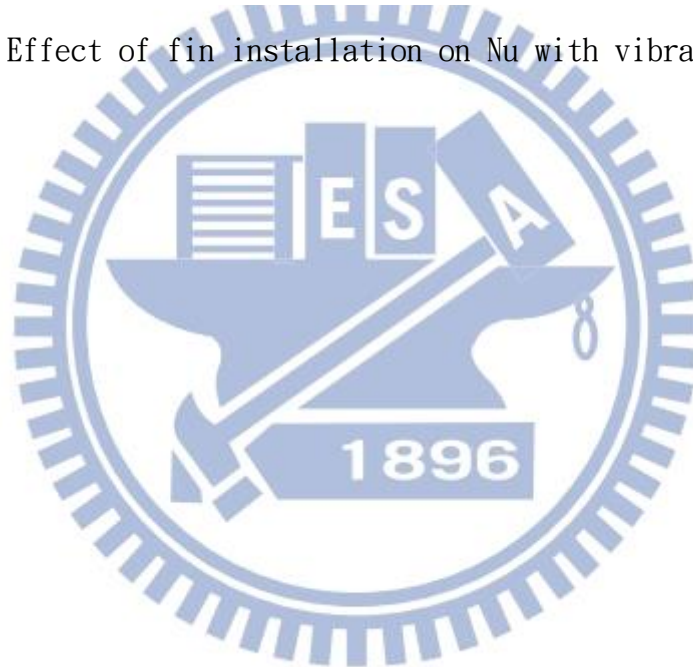


Figure 10. Effect of fin installation on Nu with vibrations ($f=2\text{Hz}$)



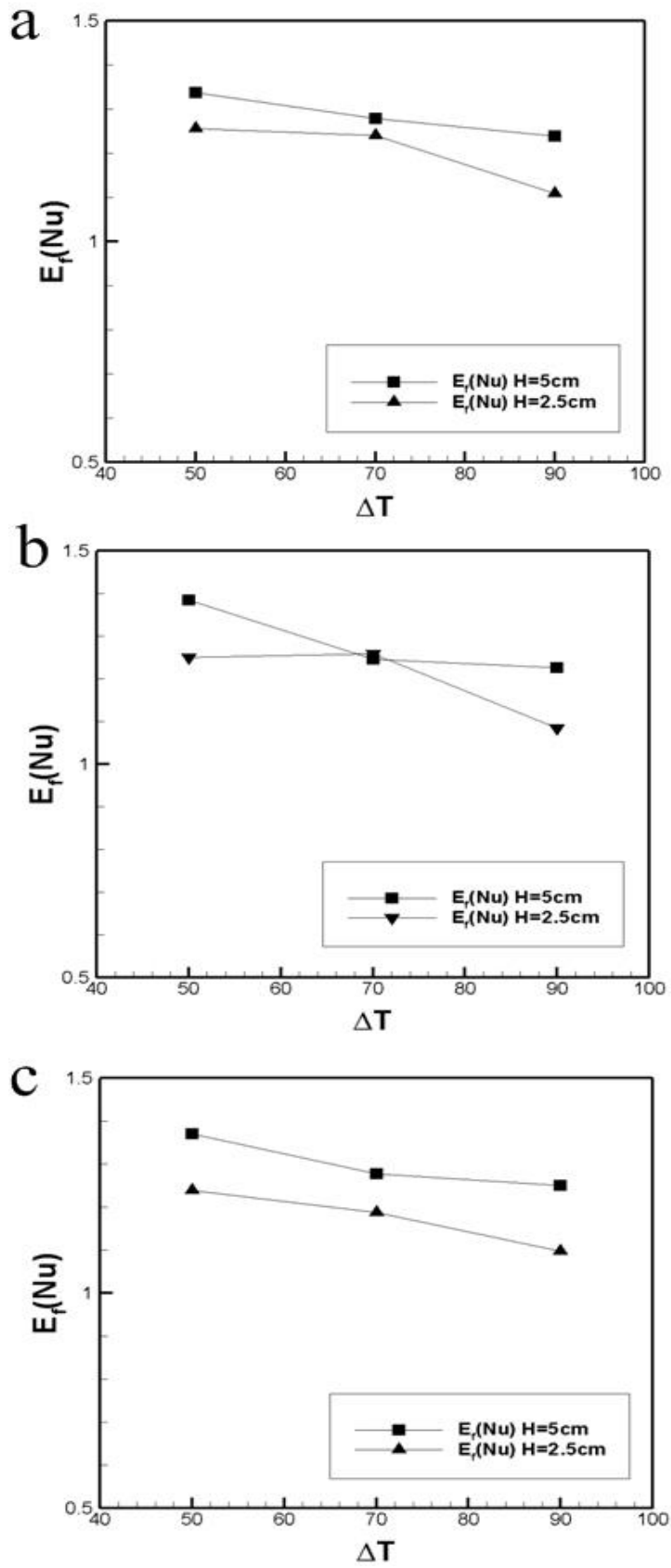


Figure 11. The $E_f(Nu)$ in different H for (a) $f=0$ (b) $f=1\text{Hz}$ (c) $f=2\text{Hz}$

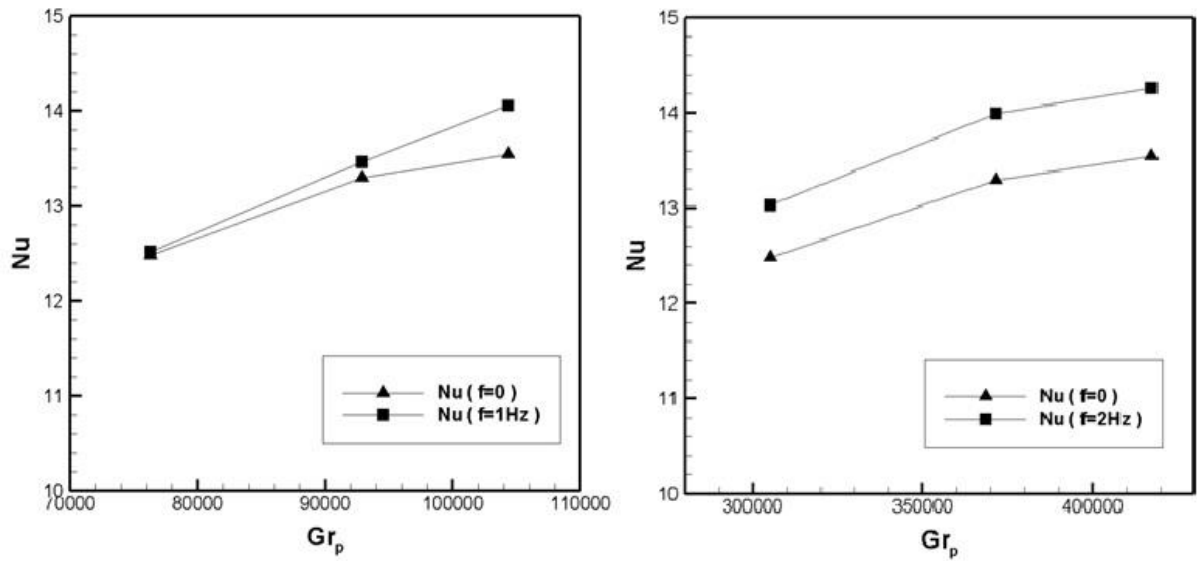


Figure 12. Effect of mechanical vibrations on Nu with smooth base plate (H=5cm)

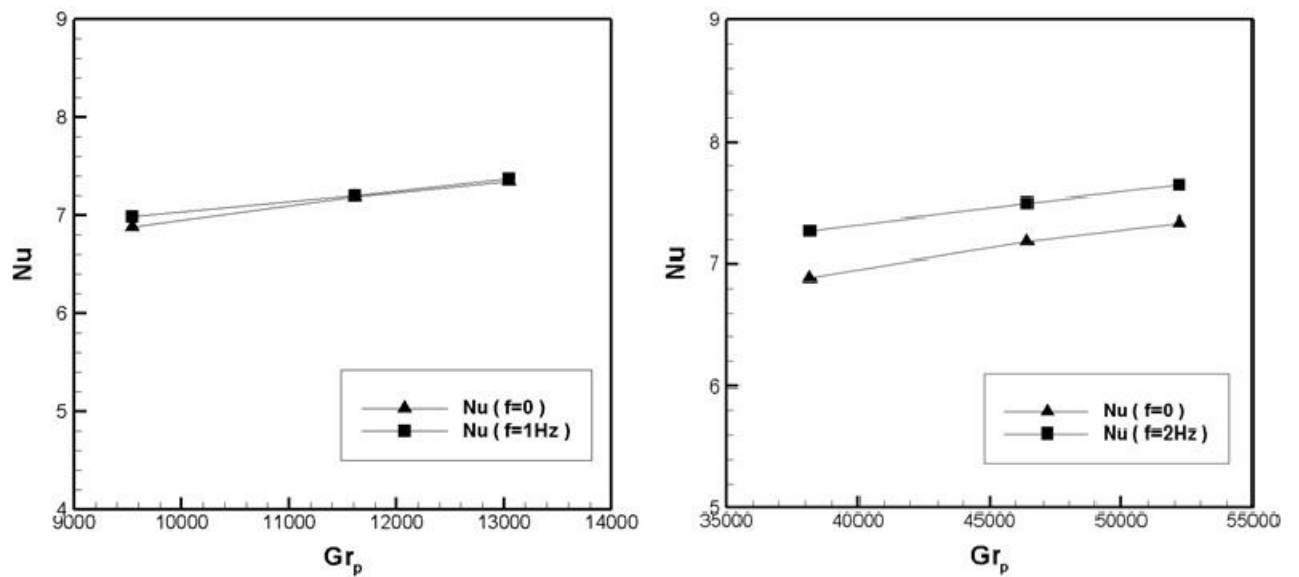
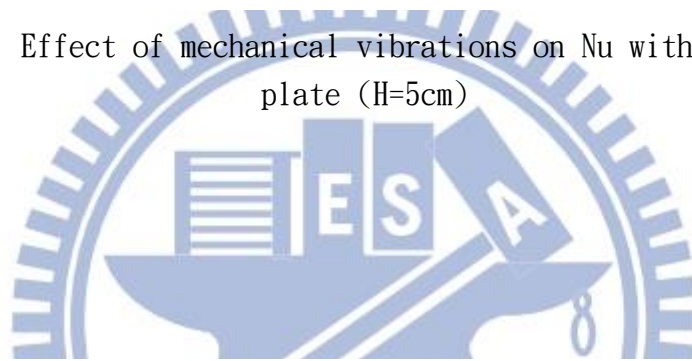


Figure 13. Effect of mechanical vibrations on Nu with smooth base plate (H=2.5cm)

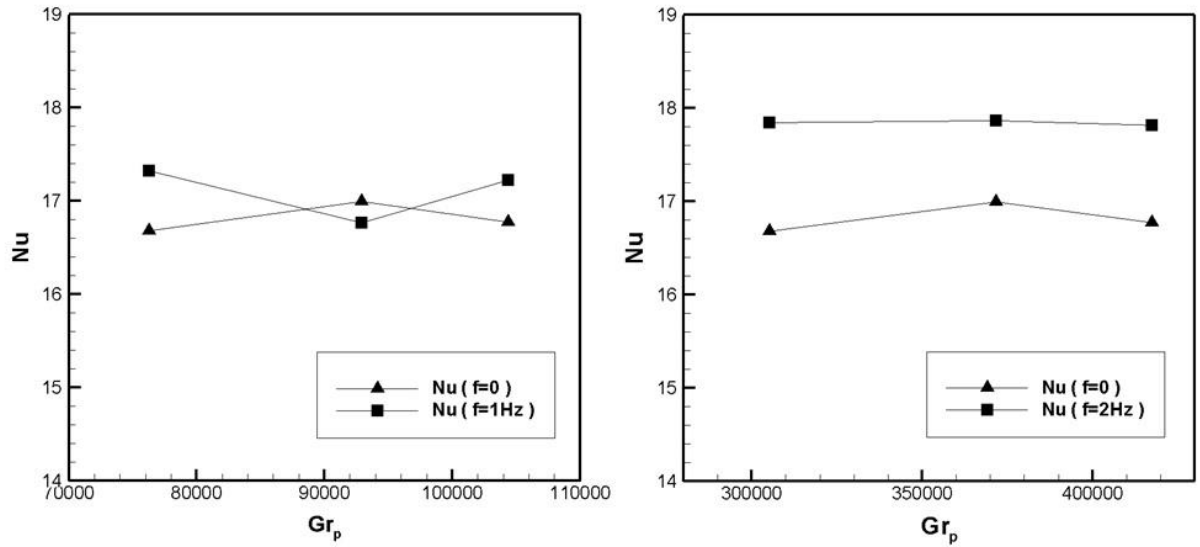


Figure 14. Effect of mechanical vibrations on Nu with finned base plate (H=5cm)

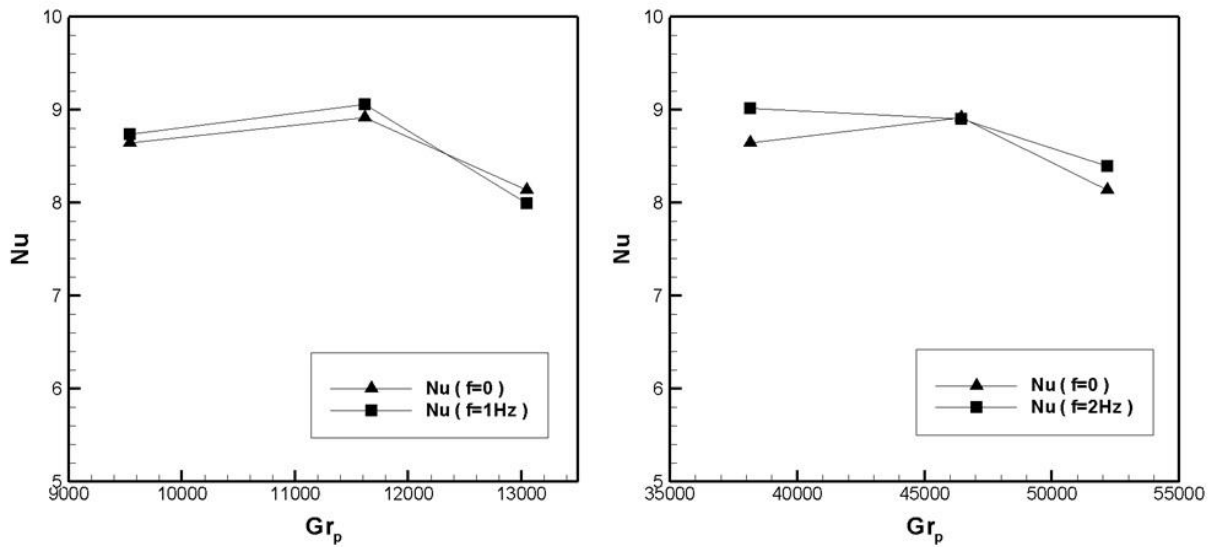
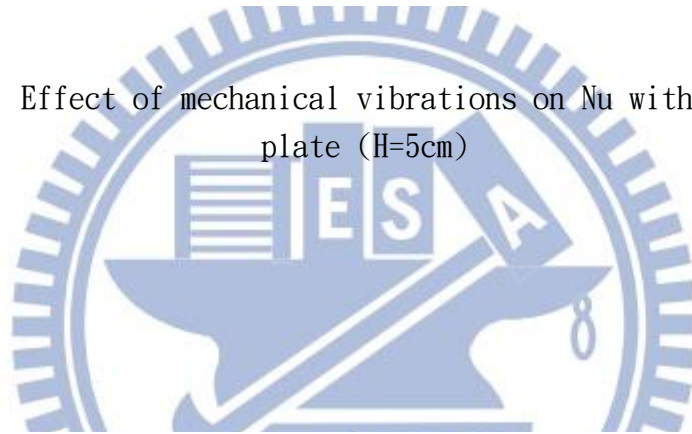


Figure 15. Effect of mechanical vibrations on Nu with finned base plate (H=2.5cm)

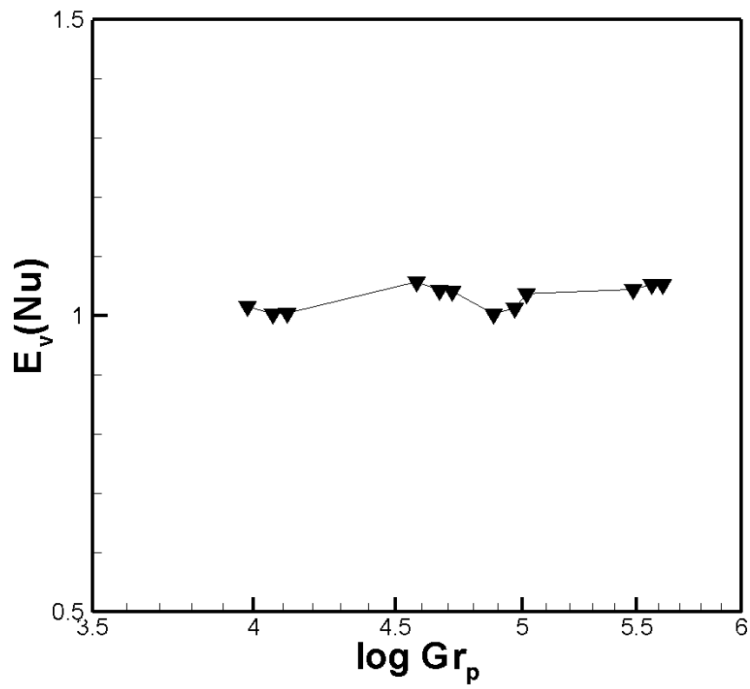


Figure 16. The $E_v(Nu)$ in different Gr_p with smooth base plate

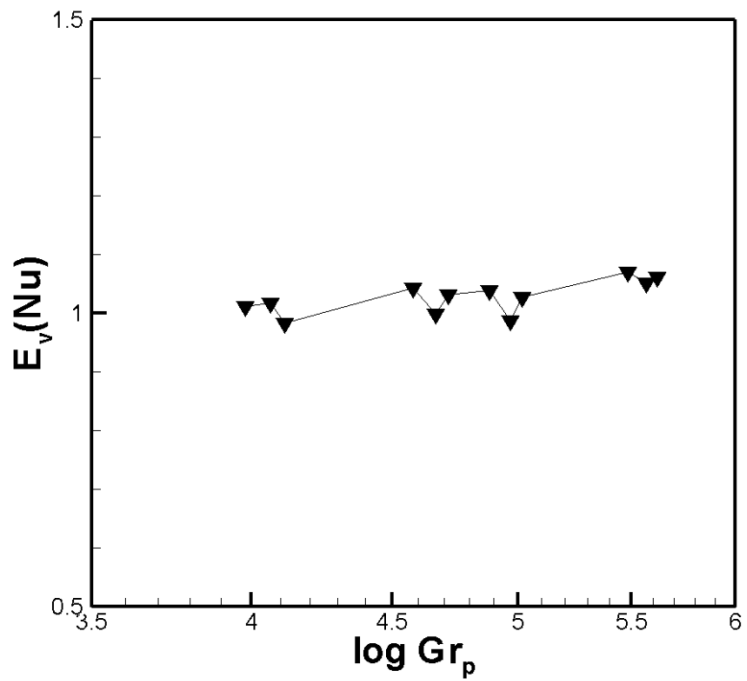


Figure 17. The $E_v(Nu)$ in different Gr_p with finned base plate

Parameter	Uncertainty
I	± 0.01 A
k	± 0.01 W/m · K
L, H	± 0.1 mm
R	± 0.1 Ω
ΔT	± 0.3 °C
ε	± 5 %
ν	± 5 %
Ra	± 7.2 %
Nu	± 8 %

Table 1. Uncertainties in test parameters

T_w (°C)	H (cm)	f (Hz)	$E_f(Nu)$	vibrations
70	2.5	0	1.256	No
90	2.5	0	1.240	No
110	2.5	0	1.108	No
70	5	0	1.337	No
90	5	0	1.278	No
110	5	0	1.238	No

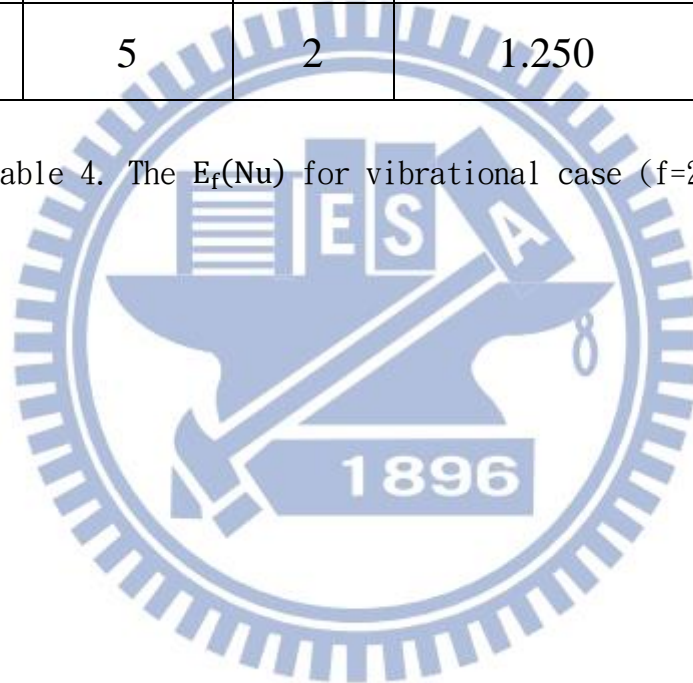
Table 2. The $E_f(Nu)$ for stationary case (f=0)

T_w (°C)	H (cm)	f (Hz)	$E_f(Nu)$	vibrations
70	2.5	1	1.250	Yes
90	2.5	1	1.258	Yes
110	2.5	1	1.085	Yes
70	5	1	1.384	Yes
90	5	1	1.246	Yes
110	5	1	1.226	Yes

Table 3. The $E_f(Nu)$ for vibrational case (f=1Hz)

T_w (°C)	H (cm)	f (Hz)	$E_f(Nu)$	vibrations
70	2.5	2	1.239	Yes
90	2.5	2	1.187	Yes
110	2.5	2	1.098	Yes
70	5	2	1.370	Yes
90	5	2	1.277	Yes
110	5	2	1.250	Yes

Table 4. The $E_f(Nu)$ for vibrational case (f=2Hz)



T_w (°C)	H (cm)	f (Hz)	$E_v(Nu)$	fin
70	2.5	1	1.015	smooth
90	2.5	1	1.002	smooth
110	2.5	1	1.004	smooth
70	2.5	2	1.057	smooth
90	2.5	2	1.044	smooth
110	2.5	2	1.042	smooth
70	5	1	1.003	smooth
90	5	1	1.013	smooth
110	5	1	1.038	smooth
70	5	2	1.044	smooth
90	5	2	1.053	smooth
110	5	2	1.053	smooth

Table 5. The $E_v(Nu)$ for smooth case

T_w (°C)	H (cm)	f (Hz)	$E_v(Nu)$	fin
70	2.5	1	1.011	finned
90	2.5	1	1.017	finned
110	2.5	1	0.983	finned
70	2.5	2	1.043	finned
90	2.5	2	0.998	finned
110	2.5	2	1.031	finned
70	5	1	1.038	finned
90	5	1	0.987	finned
110	5	1	1.027	finned
70	5	2	1.070	finned
90	5	2	1.051	finned
110	5	2	1.062	finned

Table 6. The $E_v(Nu)$ for finned case

T_w (°C)	H (cm)	f (Hz)	Nu increase due to increasing H (%)	fin
70	5	0	81.4	smooth
90	5	0	84.8	smooth
110	5	0	84.5	smooth
70	5	1	79	smooth
90	5	1	86.9	smooth
110	5	1	90.6	smooth
70	5	2	79	smooth
90	5	2	86.5	smooth
110	5	2	86.4	smooth

Table 7. The Nu increase due to increasing H for smooth cases

T_w (°C)	H (cm)	f (Hz)	Nu increase due to increasing H (%)	fin
70	5	0	93	finned
90	5	0	90.7	finned
110	5	0	106	finned
70	5	1	98.2	finned
90	5	1	85.1	finned
110	5	1	116	finned
70	5	2	98.1	finned
90	5	2	101	finned
110	5	2	112	finned

Table 8. The Nu increase due to increasing H for finned cases